J Assist Reprod Genet (2016) 33:1559–1570
DOI 10.1007/s10815-016-0798-x

GAMETE BIOLOGY

Freeze/thaw stress induces organelle remodeling and membrane recycling in cryopreserved human mature oocytes

Stefania Annarita Nottola[1] · Elena Albani[2] · Giovanni Coticchio[3,4] · Maria Grazia Palmerini[5] · Caterina Lorenzo[5] · Giulia Scaravelli[6] · Andrea Borini[3] · Paolo Emanuele Levi-Setti[2] · Guido Macchiarelli[5]

Received: 21 July 2016 / Accepted: 16 August 2016 / Published online: 1 September 2016

Abstract
Purpose Our aim was to evaluate the ultrastructure of human metaphase II oocytes subjected to slow freezing and fixed after thawing at different intervals during post-thaw rehydration.
Methods Samples were studied by light and transmission electron microscopy.
Results We found that vacuolization was present in all cryopreserved oocytes, reaching a maximum in the intermediate stage of rehydration. Mitochondria-smooth endoplasmic reticulum (M-SER) aggregates decreased following thawing, particularly in the first and intermediate stages of rehydration, whereas mitochondria-vesicle (MV) complexes augmented in the same stages. At the end of rehydration, vacuoles and MV complexes both diminished and M-SER aggregates increased again. Cortical granules (CGs) were scarce in all cryopreserved oocytes, gradually diminishing as rehydration progressed.
Conclusions This study also shows that such a membrane remodeling is mainly represented by a dynamic process of transition between M-SER aggregates and MV complexes, both able of transforming into each other. Vacuoles and CG membranes may take part in the membrane recycling mechanism.

Keywords Oocyte · Vacuoles · Organelles · Cryopreservation · Human · Ultrastructure

✉ Stefania Annarita Nottola
stefania.nottola@uniroma1.it

[1] Department of Anatomy, Histology, Forensic Medicine and Orthopaedics, Sapienza University, Rome, Italy

[2] Humanitas Research Hospital, Department of Gynecology, Division of Gynecology and Reproductive Medicine, Humanitas Fertility Center, Rozzano, Milan, Italy

[3] Tecnobios Procreazione, Centre for Reproductive Health, Bologna, Italy

[4] Present address: Biogenesi, Reproductive Medicine Centre, Monza, Italy

[5] Department of Life, Health and Environmental Sciences, University of L'Aquila, L'Aquila, Italy

[6] CNESPS, National Health Institute, Rome, Italy

Introduction

Oocyte cryopreservation currently represents a valuable procedure among assisted reproductive technologies (ART) that bypasses some ethical, moral, and religious dilemmas associated with the storage of embryos. It is a valid solution for women who have to repeat in vitro fertilization (IVF) treatments avoiding the risk of ovarian hyperstimulation syndrome, and for women who may lose their ovarian function due to surgery, cancer treatments, or premature menopause [1]. Oocyte cryostorage may also represent a possibility to counteract future infertility for healthy women who decided to postpone childbearing due to educational or socio-economic pressures (social freezing) [2]. Despite such a paramount impact of oocyte cryopreservation, the mature, metaphase II (MII) human oocyte is difficult to cryopreserve [3]. This is due to oocyte peculiar features, such as large size (low surface-to-volume ratio), high water content, elevated degree of cytoplasmic specialization, and sensitivity of the

chromosome segregation machinery [4–9]. Indeed, some structural domains of the mammalian MII oocytes, such as zona pellucida (ZP), cortical granules (CGs), and other organelles, cytoskeletal components and, particularly, meiotic spindle are sensitive to the process of cryopreservation, due to the negative effects exerted by low temperatures, formation of intracellular ice crystals, osmotic stress, and toxicity of the substances used as cryoprotectants (for references, see: [10–17]). Thus, light and transmission electron microscopy (LM and TEM) are powerful tools of investigation and evaluation of the impact that the above factors may have on human oocyte microstructure during freeze-thawing.

Vacuolization from a slight to a moderate extent is an important dysmorphism that has been frequently detected by both LM and TEM in the ooplasm of human mature oocytes subjected to cryopreservation, mainly when slow freezing is applied [12, 17, 18]. Vacuoles are also present in aging or degenerating oocytes, whereas in fresh, healthy MII oocytes they are very scarce or virtually absent [19–23]. Thus, the occurrence of vacuolization in frozen-thawed oocytes may be considered a form of structural damage explainable as a non-specific response of the oocyte to cryoinjury and/or osmotic stress. In addition, since oocytes subjected to different protocols of slow freezing may show different degrees of vacuolization [12–14, 17, 24, 25], it should not be ruled out that oocyte vacuolization may be dependent, at least in part, upon the type and/or concentration of the cryoprotectants. Oocyte dysmorphisms may be related to poor clinical outcomes [26]. Although the effects of oocyte vacuolar dysmorphism on embryo development may remain controversial [27], it is a common finding that vacuolated MII oocytes show poor fertilization rates [28]. If fertilized, vacuolated oocytes may show reduced cleavage or arrested development [22, 29, 30]. However, while oocyte vacuolization seems to be associated with IVF failure, the genesis of vacuoles and the morphodynamics of vacuole formation have not yet been fully understood.

Well-defined composite associations between mitochondria and cytoplasmic membranes are characteristically found in the ooplasm of fully grown human oocytes, named mitochondria-smooth endoplasmic reticulum (M-SER) aggregates and mitochondria-vesicle (MV) complexes [19, 22, 31, 32]. Mitochondria and associated cytoplasmic membranes may play a role in production of substances useful at fertilization and/or in rapid neoformation of membranes during early embryogenesis [20, 33, 34]. M-SER aggregates may also regulate local levels of free calcium and ATP production, thus acting on different cellular activities including the mediation of an "explosive" calcium signal at fertilization [23, 35–38]. Thus, disturbances in morphology and function of these organelle associations may lead to a reduced oocyte competence for fertilization. In this regard, the presence of very large M-SER aggregates, sometimes related to gonadotropin hyperstimulation [21], has been generally associated with compromised embryo development and implantation [39, 40], even though different opinions have been recently expressed [41–43]. On the contrary, underdeveloped M-SER aggregates have been found in a percentage of human mature oocytes subjected to vitrification [15] or to a slow freezing protocol based on the use of ethylene glycol as cryoprotectant agent [14], whereas other studies on slow-frozen oocytes treated with propanediol (PrOH) did not evidence qualitatively detectable ultrastructural alterations in M-SER aggregates [12, 13, 17]. However, a quantitative morphometric analysis on mitochondria and associated membranes has not been carried out up to now in human cryopreserved oocytes.

Several researchers, using TEM, have identified an abnormal reduction of the amount of CGs in mature oocytes of some mammals, including humans, after the application of different cryopreservation protocols [12–15, 17, 24, 44–49]. Ultrastructural evidence of premature CG release has been also found after the simple contact of the oocyte with some cryoprotectants, as described by Schalkoff et al. [50] in human oocytes exposed to either 1,2-PrOH or dimethylsulfoxide at room temperature (RT). Contrasting data have been reported by Jones et al. [51], who found an abundance of CGs in the ooplasm of human PrOH-cryopreserved oocytes, although these observations do not preclude the possibility that a partial CG exocytosis in some other areas would not be detected. Thus, keeping under observation the presence and amount of CGs in human oocytes after the freeze-thawing procedure is extremely important. In fact, precocious oocyte activation—with a consequent decrement of oocyte developmental competence—is a phenomenon that may eventually be demonstrated with the appearance of premature CG exocytosis [15].

With the aim to give a contribution in solving some questions related to the quality, timing, and entity of organelle alterations occurring during human oocyte cryopreservation, the present report was intended to evaluate presence and amount of (a) ooplasmic vacuolization, (b) organelle-specific associations such as M-SER aggregates and MV complexes, and (c) CGs in human MII oocytes subjected to slow freezing and examined after thawing, at different intervals during post-thaw rehydration. Morphological data have been collected and evaluated though an integrated LM, TEM and morphometric approach.

Materials and methods

Source of oocytes

This study was approved by Institutional Review Board of the participating Clinics. Surplus oocytes, donated for

research purpose, were obtained over a period between July 2008 and September 2010 from patients undergoing ART treatment, with high number of oocytes and after their informed consent, according to the current Italian laws. Only oocytes provided by women ($N = 32$) younger than 33 years (mean ± standard deviation, SD: 31.36 ± 1), whose infertility was due to male or disovulatory factors, were used. Controlled ovarian hyperstimulation was induced with long protocols using GnRH agonist and rFSH, according to the standard clinical procedures routinely employed by the participating Clinics [52]. Ten thousand IU of hCG were administered 36 h prior to oocyte collection. After retrieval, oocytes were cultured in IVF media (Cook IVF, Brisbane, Australia, or Sage IVF Inc, Trumbull, CT, USA). Complete removal of cumulus mass and corona cells was performed enzymatically using hyaluronidase (80 IU/ml), and mechanically by using fine bore glass pipettes. Only oocytes devoid of any dysmorphism at phase contrast microscopy (PCM) examination, showing an extruded first polar body (PBI), thus presumably at the MII stage, were assigned to the control or experimental groups. According to their assignment, oocytes were either frozen or fixed after a period of 3–4 h following retrieval.

Freezing procedure

Freezing was performed according to the two-step PrOH dehydration. In detail, the oocytes were equilibrated sequentially in solutions containing respectively 0.75 mol/l PrOH + 20 % plasma protein supplement (PPS) and 1.5 mol/l PrOH + 20 % PPS in Dulbecco's phosphate-buffered saline (PBS) (7.5 min for each step). Further, oocytes were transferred for 5 min into the loading solution (1.5 mol/l PrOH + 0.2 mol/l sucrose + 20 % PPS in PBS). Oocytes were finally loaded in plastic straws (Paillettes Crystal 133 mm; Cryo Bio System, France), individually or in small groups (maximum three oocytes per straw). Straw temperature was lowered through an automated Kryo 10 series III biological freezer (Planer Kryo 10/1,7 GB) from 20 to −8 °C at a rate of −2 °C/min). Manual seeding was performed at −8 °C. This temperature was maintained in a hold interval of 10 min in order to allow uniform ice propagation. Temperature was then decreased to −30 °C at a rate of −0.3 °C/min and finally rapidly to −150 °C at a rate of −50 °C/min. Finally, straws were directly plunged into liquid nitrogen and stored for later use.

Thawing procedure

Thawing was carried out at RT. Straws were removed from liquid nitrogen, warmed in air for 30 s and then plunged in a water bath at 37 °C for 40 s. The thawing solutions contained a gradually decreasing concentration of PrOH and a constant 0.3 mol/l sucrose concentration. Thawed oocytes were firstly released in 1.0 mol/l PrOH + 0.3 mol/l sucrose + 20 % PPS (solution 1) and incubated for 5 min. Afterwards, they were transferred in 0.5 mol/l PrOH + 0.3 mol/l sucrose + 20 % PPS (solution 2) for additional 5 min. Finally, oocytes were placed in 0.3 mol/l sucrose + 20 % PPS (solution 3) for 10 min before final dilution in PBS + 20 % PPS (solution 4) for 20 min (10 min at RT and 10 min at 37 °C). All freezing and thawing solutions were manufactured by Cook IVF, Brisbane, Australia.

Electron microscopy

Only oocytes with highest morphological scores at PCM examination [53] were selected for electron microscopy analysis. A total of 60 MII oocytes were included in this study. Fifteen of them were fixed after 3–4 h following retrieval and assigned to the control group. The other 45 oocytes, after being cultured for 4 h, were subjected to freeze-thawing as described above and fixed in glutaraldehyde after thawing, at different intervals during post-thaw rehydration, as follows: group A, oocytes fixed after the passage in thawing solution 1 ($N = 15$); group B, oocytes fixed after the passage in thawing solution 2 ($N = 15$); group C, oocytes fixed after the passage in thawing solution 3 ($N = 15$).

Oocytes were processed for LM and TEM as previously described [12–15, 54]. Oocyte fixation was performed in 1.5 % glutaraldehyde (SIC, Rome, Italy) in PBS solution. After fixation for 2–5 days at 4 °C, the samples were rinsed in PBS, post-fixed with 1 % osmium tetroxide (Agar Scientific, Stansted, UK) in PBS, and rinsed again in PBS. Oocytes were then embedded in small blocks of 1 % agar of about 5 × 5 × 1 mm in size, dehydrated in ascending series of ethanol (Carlo Erba Reagenti, Milan, Italy), immersed in propylene oxide (BDH Italia, Milan, Italy) for solvent substitution, embedded in Epoxy resin (Agar Scientific, Stansted, UK) and sectioned by a Reichert-Jung Ultracut E ultramicrotome. Semithin sections (1-μm thick) were stained with toluidine blue, examined by LM (Zeiss Axioskop) and photographed using a digital camera (Leica DFC230). Ultrathin sections (60–80 nm) were cut with a diamond knife, mounted on copper grids, and contrasted with saturated uranyl acetate followed by lead citrate (SIC, Rome, Italy). The ultrathin sections were examined and photographed using a Zeiss EM 10 and a Philips TEM CM100 Electron Microscopes operating at 80KV. Images were acquired using a GATAN charge-coupled device camera.

Ultrastructural parameters

The following parameters were evaluated by LM and TEM and taken into consideration for the qualitative morphological

assessment of the structural and ultrastructural preservation of oocytes: general features (including shape and dimensions), presence and extent of ooplasmic vacuolization, microtopography, type and quality of the organelles, integrity of the oolemma, ZP texture, and appearance of the perivitelline space (PVS) [15, 55].

PBI and MII spindle features were not systematically assessed by LM and TEM due to their detection only in sections lying on appropriate planes.

Statistical analysis

The presence of vacuoles, M-SER aggregates, and MV complexes was evaluated at the LM level on at least 3 equatorial semithin sections per oocyte (distance between the sections: 3–4 μm). For each section, counting was performed on a single panoramic image of each oocyte, obtained combining together several pictures of different oocyte portions taken at × 100 magnification by using the function Photoshop's Photomerge (PS Adobe Photoshop CS3). The amount of vacuoles, M-SER aggregates and MV complexes was expressed in number of vacuoles or organelle associations per 100 μm^2 of the oocyte area. Only structures (vacuoles, SER networks, vesicles) greater than or equal to 0.5 μm in diameter were counted.

The evaluation of CG density was performed through collection of TEM micrographs of whole surface profiles at × 6300 magnification on 3 equatorial ultrathin sections per oocyte. The images were further magnified on the PC screen to easily recognize and count CGs. Values were expressed as the number of CGs for 10 μm of the oocyte linear surface profile [12, 15, 25].

All data were expressed as mean ± SD and compared by one-way analysis of variance (ANOVA) and Tukey's test as post hoc test (GraphPad InStat). Differences in values were considered significant if $P < 0.05$.

Results

Control oocytes

A total of 15 fresh, control oocytes were observed. When analyzed by LM, these oocytes appeared rounded in shape, 90–100 μm in diameter (ZP excluded), provided with a homogeneously textured ooplasm in which vacuoles were rarely seen (Fig. 1a). Morphometric analysis revealed that the mean number ± SD of vacuoles per 100 μm^2 was 1.06 ± 0.18 in the control group (Fig. 3d). By LM and low magnification TEM the organelles, including numerous, large M-SER aggregates and small MV complexes, appeared scattered in the ooplasm (Fig. 1a, b). By morphometric analysis, the mean number ± SD of M-SER found in 100 μm^2 was 0.96 ± 0.01 while the mean number ± SD of MV in 100 μm^2 was 0.60 ± 0. 29 (Figs. 4b; 5c). A continuous, intact ZP, approximately 10–12-μm thick, completely surrounded the oocyte, which was separated from the inner zona aspect by a narrow PVS (Fig. 1a, b). By TEM, mitochondria (0.5–1 μm in diameter), rounded or oval—in relation to the orientation of the cutting section—and provided with arched *cristae*, were numerous and characteristically associated with networked SER tubules with a diameter varying from 1 to 5 μm, forming the M-SER aggregates (Fig. 1b, c). MV complexes appeared as small vesicles with a diameter of about 0.5 μm, filled with flocculent, slightly electrondense material and surrounded by mitochondria (Fig. 1b, c). Rounded, electrondense CGs, varying in diameter from 300 to 400 nm, were abundant and stratified in one/two layers in suboolemmal areas (mean number ± SD of CGs per 10 μm = 9.07 ± 0.45) (Figs. 1d; 6d).

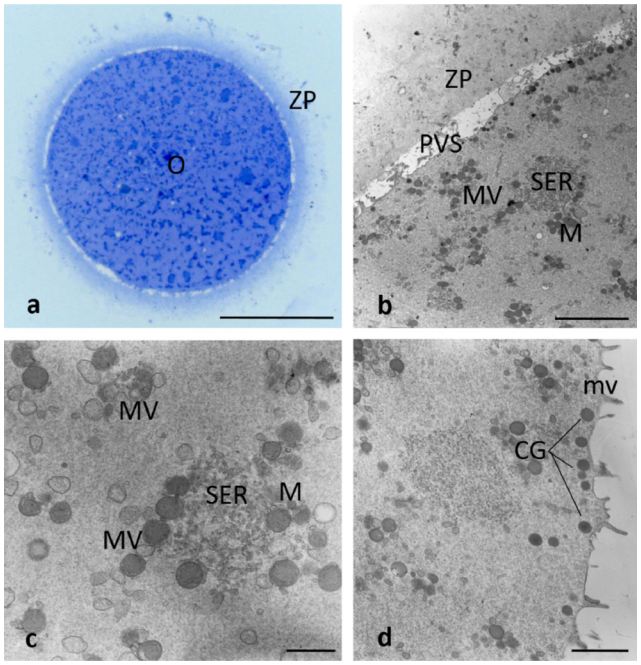

Fig. 1 Fresh human metaphase II oocytes. The general features and organelle microtopography are shown by light (Fig. 1a) and transmission (TEM) (Fig. 1b) electron microscopy. Note the rounded shape of the oocyte (*O*), the narrow perivitelline space (*PVS*), the intact zona pellucida (*ZP*) and the uniform distribution of organelles in the ooplasm. Among the organelles, numerous mitochondria (*M*), mitochondria-smooth endoplasmic reticulum (*M-SER*) aggregates and mitochondria-vesicle (*MV*) complexes can be found. By TEM, details of a M-SER aggregate and of several, small MV complexes are seen in Fig. 1c. A rim of cortical granules (CG) is also seen just beneath the oolemma in Fig. 1d. *mv* microvilli. Bar is: 45 μm (Fig. 1a); 5 μm (Fig. 1b); 1 μm (Fig. 1c); 2 μm (Fig. 1d)

Numerous microvilli of variable length projected from the oolemma into the PVS (Fig. 1d). In sections lying on appropriate planes, the PBI was detected in the PVS and the MII spindle was found in the ooplasm.

Cryopreserved oocytes

In total, 45 mature cryopreserved oocytes, 15 for each experimental group (A, B, C), were analyzed. A preliminary evaluation was performed by LM (Fig. 2a–c). All the oocytes were rounded, with a diameter ranging from 90 to 100 μm, provided with a homogeneous ooplasm and surrounded by a regular, uninterrupted ZP. No overt differences in oocyte shape/dimensions were detected between cryopreserved and control oocytes and among cryopreserved oocytes belonging to different experimental groups.

By LM, circular areas of different sizes and shapes in which staining and matter consistency were reduced, identified as vacuoles, were numerous in the ooplasm of the cryopreserved oocytes belonging to all the experimental groups (Fig. 2). With regard to their distribution, vacuoles populated both inner and outer oocyte areas, but appeared more concentrated in the deeper ooplasm. Morphometric analysis revealed that the mean number ± SD of vacuoles per 100 μm^2 was 7.20 ± 1.50 (group A), 17.05 ± 5.50 (group B), 9.50 ± 5.20 (group C). Thus, vacuoles were numerous in group A (difference between control group and group A was statistically significant, $P < 0.001$). In addition, vacuoles further increased with the progression of rehydration, reaching a maximum amount in group B (difference between groups A and B was statistically significant, $P < 0.05$) and diminishing again at the end of the rehydration process (difference between groups A and C was not statistically significant, $P = 0.3$) (Fig. 3d).

By LM and low magnification TEM, the organelles appeared evenly dispersed in the ooplasm of all frozen-thawed oocytes, as in the control samples, irrespective of the experimental group (A, B, C) (Fig. 2). However, M-SER aggregates significantly diminished following thawing, and such a decrease in number was particularly evident in the oocytes belonging to groups A and B. In fact, the mean number ± SD of M-SER was 0.20 ± 0.03 in group A (control vs group A, $P < 0.001$) and 0.04 ± 0.03 in group B (control vs group B, $P < 0.001$) (Fig. 4b). On the contrary, MV complexes, small and scarce in control oocytes, augmented in number after thawing, being especially abundant in the oocytes belonging to group B. Specifically, the mean number ± SD of MV in 100 μm^2 was 1.12 ± 0.40 in group A (control vs group A, $P < 0.05$) and 2.36 ± 0.42 in group B (control vs group B, $P < 0.001$) (Fig. 5c). At the end of the rehydration process, organelle associations showed an opposite trend: in fact, M-SER aggregates increased again in number—though never reaching the abundance shown in control oocytes—whereas MV

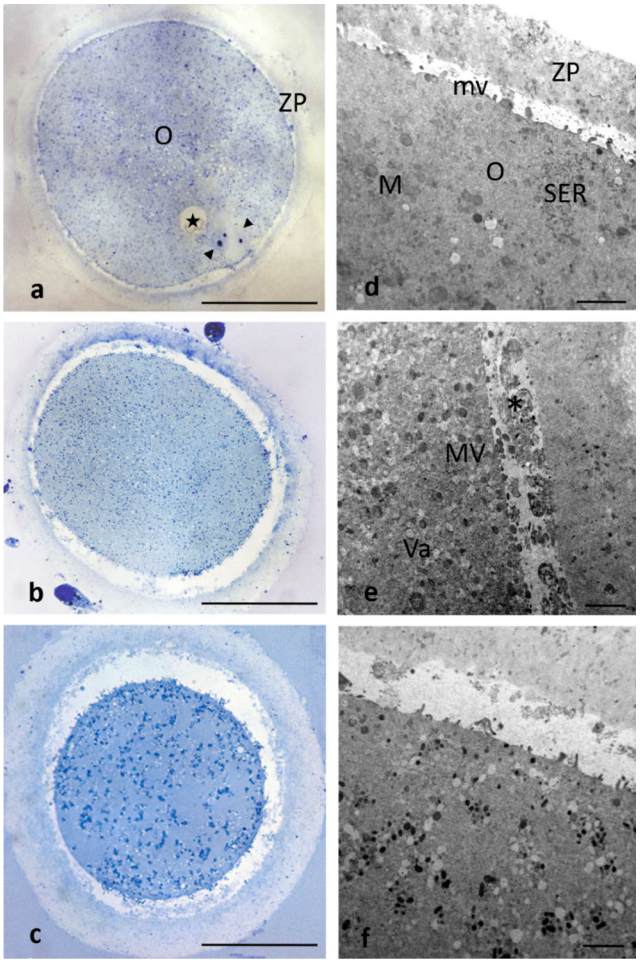

Fig. 2 Cryopreserved human metaphase II (MII) oocytes. By light (Fig. 2a–c) and transmission (Fig. 2d–f) electron microscopy, no overt difference in shape, dimensions, and organelle distribution is seen among the oocytes (*O*) belonging to group A (Fig. 2a, d), B (Fig. 2b, e), and C (Fig. 2c, f) and between fresh (see Fig. 1) and cryopreserved oocytes (Fig. 2). Note the intact zona pellucida (ZP) (Fig. 2a–c) and the presence of microvilli (*mv*) on the oolemma (Fig. 2d–f). Numerous vacuoles (*Va*) are seen in all cryopreserved oocytes, particularly abundant in group B (Fig. 2b, e). The apparent reduced dimensions, enlargement of the perivitelline space, and increased ZP thickness of the oocyte shown in Fig. 2c are effects of the section plane (not equatorial). *arrowheads* MII spindle with chromosomes, *star* large vacuole possibly due to a gas bubble, *M* mitochondria, *SER* smooth endoplasmic reticulum, *MV* mitochondria-vesicle complexes, *asterisk* remnants of the first polar body. Bar is: 45 μm (Fig. 2a); 40 μm (Fig. 2b); 35 μm (Fig. 2c); 2 μm (Fig. 2d–f)

complexes diminished in the oocytes belonging to group C, being respectively 0.87 ± 0.05 (control vs group C, $P < 0.001$) and 0.67 ± 0.29 (control vs group C, $P = 0.6$) (Figs. 4b; 5c).

By TEM, vacuoles, ranging in size from 0.5 to 4 μm, appeared delimited by membranes that were at times interrupted and characterized, in some parts, by densely organized indentations or niches. The inside of these compartments was scarcely electron-dense in comparison to the surrounding cytoplasm and occasionally contained cell debris (Fig. 3a–c).

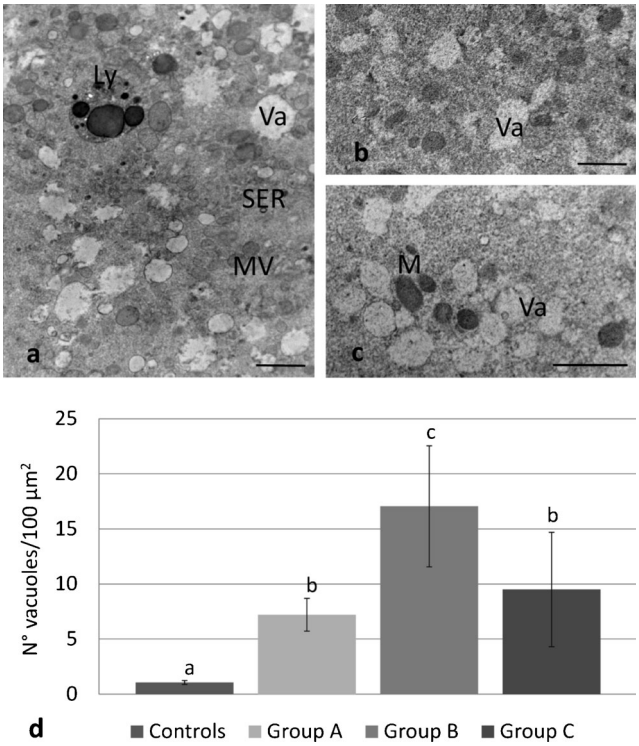

Fig. 3 Cryopreserved human metaphase II oocytes. By transmission electron microscopy, vacuoles (*Va*) are present in the ooplasm of the cryopreserved oocytes belonging to group A (Fig. 3a), B (Fig. 3b), and C (Fig. 3c). Vacuoles appear empty (Fig. 3a–c) and may be delimited by a discontinuous membrane (Fig. 3a). A close association between vacuoles and lysosomes (*Ly*) is seen in Fig. 3a. Mitochondria (*M*), smooth endoplasmic reticulum (*SER*) networks and mitochondria-vesicle (*MV*) complexes are seen in the areas among vacuoles (Fig. 3a, c). Note the increased density of the cytoplasmic matrix in group b (Fig. 3b) in comparison with fresh controls (Fig. 1b–d) and groups a and c (Fig. 3a, c). Bar is: 1 μm (Fig. 3a–c). Fig. 3d: Number of vacuoles (vacuole diameter ≥ 0.5 μm) per 100 μm^2 of oocyte area. Values for each group are expressed as mean ± SD. *Different letters* indicate significant differences ($P < 0.05$)

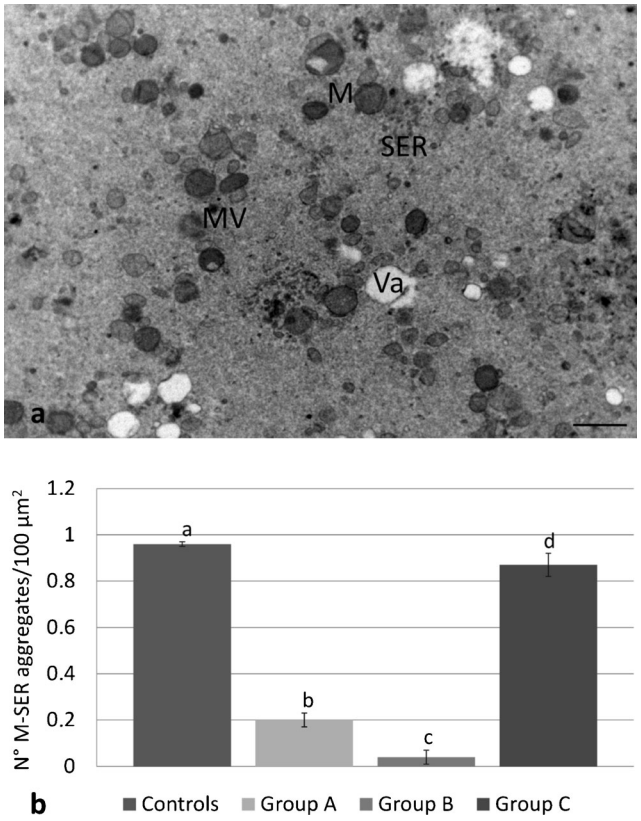

Fig. 4 Cryopreserved human metaphase II oocytes. Oocyte belonging to group A, a representative, panoramic picture of the ooplasm, as seen by transmission electron microscopy (Fig. 4a). Note the presence of typical mitochondria-smooth endoplasmic reticulum (*M-SER*) aggregates, together which numerous mitochondria (*M*) and mitochondria-vesicle (*MV*) complexes. *Va* vacuoles. Bar is: 1 μm (Fig. 4a). Fig. 4b: Number of M-SER aggregates (SER network diameter ≥ 0.5 μm) per 100 μm^2 of oocyte area. Values for each group are expressed as mean ± SD. *Different letters* indicate significant differences ($P < 0.05$)

Sometimes, secondary lysosomes were found in the proximity of the vacuoles (Fig. 3a). In the group B, the more pronounced vacuolization was often associated with an increased density of the cytoplasmic matrix (Fig. 3b).

A normal pattern of organelles was usually detected by TEM in ooplasm of the cryopreserved oocytes belonging to all experimental groups, including the ooplasmic areas adjacent to vacuoles (Figs. 3a,c; 4a). With this regard mitochondria, M-SER aggregates and MV complexes did not show overt qualitative ultrastructural changes if compared to those organelles and organelle associations found in control oocytes (Figs. 4a; 5a,b, inset). However, a percentage of small M-SER aggregates was found (with a diameter of SER networks of 1–2 μm), particularly in the oocytes belonging to groups A and B, whereas unusually large MV complexes (up to 2.5 μm in vesicular diameter) were sometimes found in the oocytes belonging to group B.

TEM analysis also revealed that CGs were scanty, arranged in a discontinuous layer, and sometimes scarcely electrondense in the cryopreserved oocytes belonging to all experimental groups in respect to those found in the control group (Fig. 6a–c). In addition, when a morphometric evaluation was performed, the mean number ± SD of CGs per 10 μm was 6.28 ± 1.12 (group A), 3.17 ± 0.28 (group B), 2.33 ± 0.50 (group C), suggesting that CGs underwent an initial reduction at the beginning of rehydration (difference between control group and group A was statistically significant, $P < 0.001$) and further decreased in number as rehydration progressed (differences between groups A and B and between groups B and C were statistically significant, $P < 0.001$ and $P < 0.05$, respectively) (Fig. 6d).

Numerous microvilli were also seen bordering the oolemma and projecting into the PVS (Figs. 2d–f; 6a–c). In sections lying on appropriate planes, the PBI was detected in the PVS and the MII spindle was found in the ooplasm.

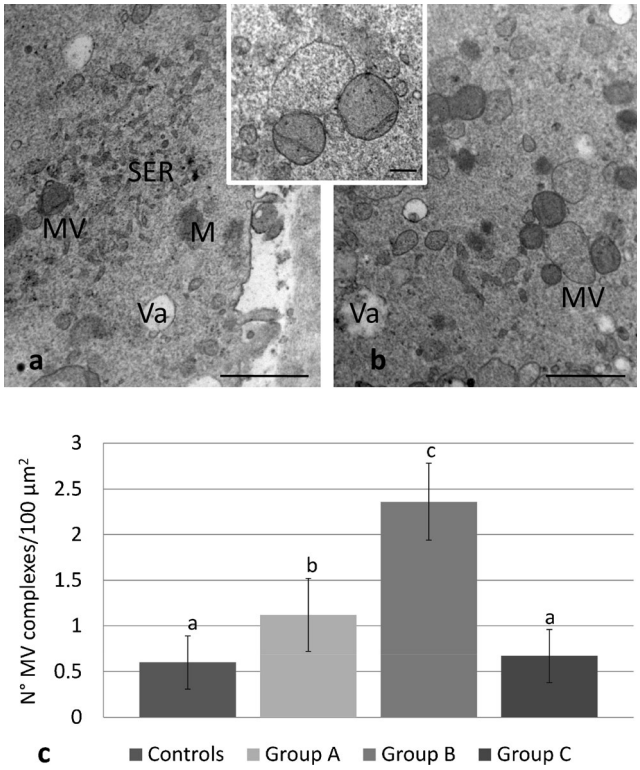

Fig. 5 Cryopreserved human metaphase II oocytes. Oocytes belonging to group A, representative pictures of mitochondria (*M*), mitochondria-smooth endoplasmic reticulum (*M-SER*) aggregates and mitochondria-vesicle (*MV*) complexes, as seen by transmission electron microscopy (Fig. 5a, b, inset). Note the presence of well preserved mitochondria and of typical MV complexes of various sizes. A high magnification of a MV complex is shown in the inset. Differently from vacuoles, the vesicles belonging to MV complexes are filled with a slightly electrondense material, are surrounded by an intact membrane and are closely associated to mitochondria. *Va* vacuoles. Bar is: 1 μm (Fig. 5a, b); 0.2 μm (inset). Fig. 5c: Number of MV complexes (vesicle diameter ≥ 0.5 μm) per 100 μm² of oocyte area. Values for each group are expressed as mean ± SD. *Different letters* indicate significant differences ($P < 0.05$)

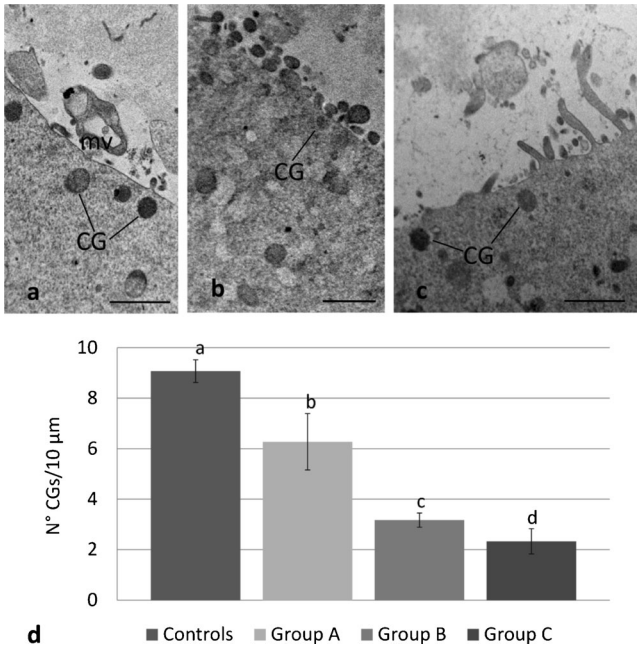

Fig. 6 Cryopreserved human metaphase II oocytes. In cryopreserved oocytes belonging to group A (Fig. 6a), B (Fig. 6b), and C (Fig. 6c), cortical granules (CG) appear by transmission electron microscopy sparse or isolated, forming a discontinuous layer. *mv* microvilli. Bar is: 1 μm (Fig. 6a–c). Fig. 6d: Number of CGs per 10 μm of oocyte linear surface profile. Values for each group are expressed as mean ± SD. *Different letters* indicate significant differences ($P < 0.05$)

Discussion

In humans, numerous studies suggest that post-thaw survival rates of oocytes that have undergone slow freezing are inferior to those of oocytes subjected to vitrification procedures [56]. In addition, oocyte vitrification, compared to slow freezing, probably increases implantation and pregnancy rates [57, 58]. The results, however, as reported in the Italian ART registry, are not homogeneous among clinics and protocols [59] since there is a wide variation in pregnancy rates among different centers [58]. Further, as it results from a general survey of the literature, the total number of women and pregnancies in the included trials were low and the evidence was limited by imprecision [57]. Moreover, ultrastructural dysmorphisms have been identified in both vitrified-warmed and frozen-thawed human MII oocytes, although at a different extent [17].

In this regard, while vitrification seems to have a clear role in ART, continued research to establish optimal slow freezing methods for human MII oocytes seems required, which may assist in alleviating concerns over safety issues related to vitrification, such as storage, transport and the use of very high cryoprotectant concentrations [60]. Slow freezing of oocytes can thus be a still valid tool in IVF practice when performed with a suitable protocol [61, 62].

The purpose of this study was firstly to investigate the phenomenon of vacuolization in human MII oocytes subjected to slow freezing, since presence and extent of this ultrastructural dysmorphism can be an important indicator of oocyte quality after cryopreservation. Secondly, we aimed to assess in the same oocytes the morphodynamics of typical oocyte organelles and organelle associations (M-SER aggregates, MV complexes, CGs) during freeze-thawing.

In particular, this is the first comprehensive study that describes in detail, from both a qualitative and quantitative point of view, the structural and ultrastructural modifications occurring just after thawing, during the rehydration steps. In fact, although several factors have been successfully optimized in the protocols used to cryopreserve human oocytes, up to now, post-thaw rehydration conditions received a limited attention [5, 63, 64]. Different rehydration conditions seem also to influence the survival of vitrified-warmed human oocytes [65]. Rehydration could, indeed, sensitize the oocyte and make it

particularly vulnerable, since removal of the intracellular cryoprotectant and the re-establishment of the original water content occurring during this procedure are both sources of osmotic stress for the cell. In this view, it seems essential to know in detail in which step/steps of the rehydration procedure cryoinjuries may occur, in order to optimize rehydration conditions, too.

General features

All the oocytes showed similar shape, dimensions, and overall appearance, irrespective of their classification (control or experimental groups A, B, and C). Thus, neither freezing nor thawing, including the different steps of post-thaw rehydration, seemed to associate with any significant variation in volume and/or general appearance of the oocytes. This feature well correlates with previous observations on human mature oocytes subjected to different protocols of slow freezing [12–14, 17] or vitrification [15, 17, 55, 66], further emphasizing that current cryopreservation protocols do not significantly impair oocyte general architecture.

By LM and TEM, the organelles appeared uniformly dispersed in the ooplasm of all the oocytes. However, organelle-specific differences were found between control and frozen-thawed oocytes as extent of vacuolization and differences in the number of M-SER aggregates, MV complexes, and CGs.

Vacuoles

We found a slight to moderate vacuolization in the cryopreserved oocytes belonging to all experimental groups. Vacuoles were instead only occasionally present in the ooplasm of fresh oocytes. In particular, vacuoles were already found in the group A, after oocyte exposure to the thawing solution 1, suggesting that they may form during freezing and/or at thawing. Further, vacuoles increased in number as post-thaw rehydration proceeded. They reached a maximum amount in group B, after oocyte exposure to the thawing solution 2, which contains the lowest concentration of PrOH during PrOH step-wise dilution. Finally, vacuoles decreased again in number at the end of the rehydration process (group C), after oocyte exposure to the thawing solution 3, which is PrOH-free. A measurable number of vacuoles, however, remain in the ooplasm of frozen-thawed oocytes, indicating that their recovery is largely incomplete.

The abundance of vacuoles in frozen-thawed oocytes can be interpreted as a manifestation of oocyte stress during cryopreservation. As introduced above, the degree of oocyte vacuolization significantly increases by applying slow freezing [12–14, 17, 67], whereas data on the presence of vacuoles in vitrified oocytes appear still undefined and controversial [15, 17, 66–68]. Taken together, however, all these data indicate that vacuoles are less represented in vitrified than in slow-frozen oocytes.

Vacuoles may derive from swelling and coalescence of Golgi and/or SER membranes [21, 69], possibly associated to cytoskeletal defects [14, 22]. In the mature oocyte SER membranes, when transforming into vacuoles, become interrupted and lose their close association with mitochondria, typical for M-SER aggregates and MV complexes, acquiring degenerative features [38]. Disruption of such a "molecular hug" between mitochondria and SER [70] may contribute to the occurrence of altered calcium transients in cryopreserved oocyte. Peripheral vacuoles may also originate from oolemmal invaginations [66] and/or clusters of endocytotic vesicles forming in the oocyte cortex, as it occurs in oocytes exposed to cryoprotectants only [12, 50]. In cryopreserved oocytes vacuoles could also derive from altered, swollen mitochondria [46, 47] or from the fusion of degenerating CGs, associated to an extensive loss of the electron-dense granule content [48].

In this study, we sometimes identified secondary lysosomes adjacent to vacuoles. Vacuoles and lysosomes may fuse, forming structures with a mixed content involved in the degradation of ooplasmic material via autophagy [71]. Some authors recently hypothesize that autophagic activation in cryopreserved oocytes could be a natural, adaptative response to "cold" stress [72, 73].

In addition, we found that the more marked vacuolization of the oocytes belonging to group B was often associated with an increased density of the ooplasm. All these features are similar to those found in post-mature, atretic oocytes unfertilized after in vitro insemination [20]. This is a further prove that regressive changes in cryopreserved oocytes are consequent to altered cytoplasmic dynamics that are particularly expressed when the cryoprotectant PrOH reaches its lowest concentration in the second step of rehydration.

M-SER aggregates and MV complexes

In this study, we also found that significant variations, of opposite trend, occurred during freeze-thawing in size and number of M-SER aggregates and MV complexes.

In particular, M-SER aggregates, large and abundant in the ooplasm of fresh controls, decreased in size and number after thawing, particularly in the oocytes belonging to groups A and B (first and intermediate stages of post-thaw rehydration), indicating a special sensitivity of these aggregates to cryoprotectant exposure and, particularly, to PrOH withdrawal. On the contrary, M-SER aggregates significantly increased in group C, where PrOH was completely removed from the thawing solution and a recovery of metabolic activities occurred. An opposite trend was observed for MV complexes, and these latter changes closely resemble those previously reported for vacuoles.

On the basis of these findings, we suggest that ooplasmic membranes, whose dynamic structure may be regulated by cytoskeletal activity, as occurs in other cells [74], become capable of transforming into each other under an appropriate stimulus. According to this view, SER elements could dynamically acquire different shapes (tubules or vesicles) depending on the metabolic/structural needs of the cell, actually belonging to the same system of interconnected membranes. In fact, transitional figures with intermediate characteristics between tubules and vesicles have been observed by TEM [20]. In particular, we speculate that M-SER aggregates and small MV complexes, commonly found in the ooplasm of MII oocytes before freezing, can both give rise to numerous, large MV complexes after thawing and during rehydration, through a generous SER membrane reassembly. This is confirmed by previous studies in which the authors suggested that aging and/or prolonged culture can elicit a similar transition into the oocyte [17, 20, 38]. Large MV complexes are also present in GV oocytes that have reached MII stage after 24-h culture (in vitro matured oocytes) [75, 76]. Therefore, M-SER to MV transition does not seem related only to aging or culture period but can be also induced in cryopreserved oocytes by step-wise dilution of PrOH during post-thaw rehydration.

In this study, we also originally reported through a morphological approach that a reversal of this phenomenon of membrane "recycling" occurs at the end of freeze-thawing, when the rehydration process is completed and culture conditions regain a more physiological state. As a consequence of this, the large vesicular component of MV complexes could shrink again to form small vesicles and tortuous, anastomosing SER tubules of M-SER aggregates. This well correlates with previous reports on human oocytes subjected to slow freezing and treated with PrOH, which did not evidence at the end of the procedure of slow freezing any qualitative ultrastructural change of these aggregates in respect to fresh controls [12, 13, 17]. However, from a quantitative morphometric analysis, we hereby reported a complete recovery only for MV complexes, whereas M-SER aggregates do not reach the number found in fresh controls, thus undergoing a reliable but partial recovery at the end of the rehydration process.

Cryopreservation has been reported to affect calcium oscillation in the human oocytes [77]. In this vein, since, as reported above, calcium levels in the oocyte are regulated by a correct cross-talk between mitochondria and associated ooplasmic membranes, membrane reassembling during rehydration may produce altered, although temporary, calcium transients, possibly interfering with oocyte competence to fertilization.

It seems also worth noting that, irrespective of the above described diffuse recycling of ooplasmic membranes, associated mitochondria appear concerned neither by freezing nor by thawing and its sequential post-thaw rehydration steps, maintaining unaltered their ultrastructure. This finding further reinforces the concept that both slow freezing and vitrification procedures do not significantly affect mitochondrial structure in human MII oocytes [12–15, 17].

Finally, on the basis of what discussed above, we cannot rule out that vacuoles and their membranes can play an active role in the membrane recycling that occurs during freeze-thawing. In fact, the membranes of M-SER aggregates and MV complexes could sometimes derail during their reassembling, becoming oriented toward vacuole transformation.

Cortical granules

In this study, we revealed that CGs were scarce in the oocytes belonging to all experimental groups in respect to those found in the fresh control group. CGs gradually diminished as post-thaw rehydration progressed, reaching their lowest concentration in group C and, thus, revealing the occurrence of a gradual but progressive loss during freeze-thawing. This feature well correlates with previous reports in which an ubiquitous reduction in number of CGs was found at the end of the cryopreservation procedure, irrespective of the protocol applied (slow freezing, vitrification with closed or open devices) [12–15, 17]. A reduced amount and electrondensity of CGs in cryopreserved oocytes may be due to the occurrence of a premature exocytosis of the CG content into the PVS with the consequent hardening of the inner aspect of the ZP, thus impairing oocyte fertilizability.

The novelty of our observations on CG morphodynamics during cryopreservation is related to the following considerations. Firstly, the whole freeze-thawing procedure may induce CG loss during cryopreservation. The reduction of CGs was in fact already evident in oocytes from group A. This means that the CG release could begin during freezing and/or at thawing. Secondly, the further reduction of CG observed in groups B and C indicates that the CG exocytosis does not stop after thawing, but continues throughout the following phases of rehydration. Such CG loss is thus the only phenomenon, among those described in this study, apparently not subjected to any kind of recovery.

Several studies have shown that the mere exposure of mature oocytes to cryoprotectants leads to a reduction in the number and electron-density of CGs [24, 50]. Therefore, also on the basis of these reports, we can further emphasize that the progressive CG loss reported in this study may be related not only to low temperatures but also to the processes of cryoprotectant addition (dehydration step) and removal (rehydration step). Cryoprotectant (PrOH) addition, in particular, has been reported to have a role in inducing a precocious oocyte activation, and consequent CG exocytosis, by increasing calcium intake [25, 78]. More recently, Gualtieri et al. observed a significant delay of the recovery of intracellular calcium to basal levels in frozen-thawed oocytes [67]. According to the results

obtained in our work, it can be assumed that the concentration of cytosolic calcium, once altered during dehydration, may further increase during the rehydration and consequent PrOH withdrawal, thus resulting in the described continuous, progressive CG release.

In addition, the gradual loss of CGs during freeze-thawing leads us to hypothesize that the membranes of the exocytosed granules may not only be reintegrated in the oolemma but may also, at least in part, contribute to the above described ooplasmic membrane recycling.

Conclusions and future perspectives

In this report, we have originally reported that oocyte ultrastructural dysmorphisms related to cryopreservation and possibly responsible of low oocyte fertilizability not only occur during freezing and thawing, in a strict sense, but also during post-thaw rehydration. These cellular alterations, induced by low temperatures and by osmotic and chemical forces produced during cycles of dehydration-rehydration as well, may alter the distribution and activity of oocyte cellular components.

In particular, although slow freezing appears to ensure a good overall preservation of the oocyte; nevertheless, vacuolization and CG release remain crucial limits. It seems also worth noting that all systems of ooplasmic membranes appear significantly affected by freeze-thawing but, except for CGs, their alterations seem to undergo a partial or, more rarely, an almost complete recovery after thawing, at the end of the rehydration process. In addition, the observed variations in the number of M-SER aggregates and MV complexes, occurring during freeze-thawing, suggest that a dynamic process of transition between these two forms of organelle associations may occur. At this regard, it should not be excluded that vacuole and CG membranes, and oolemma as well, may take part in the recycling mechanism. Such shuttle of membranes, starting during freezing and/or at thawing but mainly occurring during rehydration, may be related to alterations of the cytoskeletal stiffness [79] presumably due to PrOH administration and/or withdrawal [80, 81]. We cannot exclude, of course, that the described membrane restructuring is also related to calcium disturbances. From a merely morphological point of view, this recycling reveals a sort of morphogenetic multipotence of the oocyte cytomembranes, possibly eliciting membrane turnover and delivery or clearance of substances (CG content, cryoprotectants, calcium, other solutes?), as postulated for other cells [82].

Finally, a similar ultrastructural approach could be applied in the future to the study of the rehydration process in slow-frozen oocytes undergoing rapid warming [62] and in vitrified-warmed oocytes belonging to both conventional and low-cryoprotectant vitrification protocols [83].

Acknowledgments The present study was supported by grants from the National Health Institute, Italian Ministry of Health and the Italian Ministry of Education, University and Research (grants from *Sapienza* University, Rome and University of L'Aquila, L'Aquila). The Authors wish to acknowledge Mr. Ezio Battaglione of the Laboratory for Electron Microscopy "Pietro M Motta," Department of Anatomy, Histology, Forensic Medicine and Orthopaedics, *Sapienza* University, Rome, for his contribution to sample preparation.

Compliance with ethical standards All procedures performed in studies involving human participants were in accordance with the ethical standards of the institutional and/or national research committee and with the 1964 Helsinki declaration and its later amendments or comparable ethical standards.

Conflict of interest The authors declare that they have no conflict of interest.

References

1. Cil AP, Seli E. Current trends and progress in clinical applications of oocyte cryopreservation. Curr Opin Obstet Gynecol. 2013;25:247–54.
2. Lockwood GM. Social egg freezing: the prospect of reproductive 'immortality' or a dangerous delusion? Reprod Biomed Online. 2011;23:334–40.
3. Hosseini SM, Nasr-Esfahani MH. What does the cryopreserved oocyte look like? A fresh look at the characteristic oocyte features following cryopreservation. Reprod Biomed Online. 2016;32:377–87.
4. Van Blerkom J, Davis PW. Cytogenetic, cellular, and developmental consequences of cryopreservation of immature and mature mouse and human oocytes. Microsc Res Tech. 1994;27:165–93.
5. Coticchio G, Bonu MA, Sciajno R, Sereni E, Bianchi V, Borini A. Truths and myths of oocyte sensitivity to controlled rate freezing. Reprod Biomed Online. 2007;15:24–30.
6. Gardner DK, Sheehan CB, Rienzi L, Katz-Jaffe M, Larman MG. Analysis of oocyte physiology to improve cryopreservation procedures. Theriogenology. 2007;67:64–72.
7. Gook DA, Edgar DH. Human oocyte cryopreservation. Hum Reprod Update. 2007;13:591–605.
8. Lornage J, Salle B. Ovarian and oocyte cryopreservation. Curr Opin Obstet Gynecol. 2007;19:390–4.
9. Clark NA, Swain JE. Oocyte cryopreservation: searching for novel improvement strategies. J Assist Reprod Genet. 2013;30:865–75.
10. Coticchio G, De Santis L, Rossi G, Borini A, Albertini D, Scaravelli G, et al. Sucrose concentration influences the rate of human oocytes with normal spindle and chromosome configurations after slow-cooling cryopreservation. Hum Reprod. 2006;21:1771–6.
11. Coticchio G, Bromfield JJ, Sciajno R, Gambardella A, Scaravelli G, Borini A, et al. Vitrification may increase the rate of chromosome misalignment in the metaphase II spindle of human mature oocytes. Reprod Biomed Online. 2009;19 Suppl 3:29–34.
12. Coticchio G, Borini A, Distratis V, Maione M, Scaravelli G, Bianchi V, et al. Qualitative and morphometric analysis of the ultrastructure of human oocytes cryopreserved by two alternative slow cooling protocols. J Assist Reprod Genet. 2010;27:131–40.
13. Nottola SA, Macchiarelli G, Coticchio G, Bianchi S, Cecconi S, De Santis L, et al. Ultrastructure of human mature oocytes after slow cooling cryopreservation using different sucrose concentrations. Hum Reprod. 2007;22:1123–33.

14. Nottola SA, Coticchio G, De Santis L, Macchiarelli G, Maione M, Bianchi S, et al. Ultrastructure of human mature oocytes after slow cooling cryopreservation with ethylene glycol. Reprod Biomed Online. 2008;17:368–77.
15. Nottola SA, Coticchio G, Sciajno R, Gambardella A, Maione M, Scaravelli G, et al. Ultrastructural markers of quality in human mature oocytes vitrified using cryoleaf and cryoloop. Reprod Biomed Online. 2009;19 Suppl 3:17–27.
16. Bromfield JJ, Coticchio G, Hutt K, Sciajno R, Borini A, Albertini DF. Meiotic spindle dynamics in human oocytes following slow-cooling cryopreservation. Hum Reprod. 2009;24:2114–23.
17. Bianchi V, Macchiarelli G, Borini A, Lappi M, Cecconi S, Miglietta S, et al. Fine morphological assessment of quality of human mature oocytes after slow freezing or vitrification with a closed device: a comparative analysis. Reprod Biol Endocrinol. 2014;12:110.
18. Camboni A, Martinez-Madrid B, Dolmans MM, Amorim CA, Nottola SA, Donnez J, et al. Preservation of fertility in young cancer patients: contribution of transmission electron microscopy. Reprod Biomed Online. 2008;17:136–50.
19. Sundström P, Nilsson BO, Liedholm P, Larsson E. Ultrastructural characteristics of human oocytes fixed at follicular puncture or after culture. J In Vitro Fert Embryo Transf. 1985;2:195–206.
20. Motta PM, Nottola SA, Micara G, Familiari G. Ultrastructure of human unfertilized oocytes and polyspermic embryos in an IVF-ET program. Ann N Y Acad Sci. 1988;541:367–83.
21. Sathananthan AH, Ng S-C, Bongso A, Trounson A, Ratnam S. Visual atlas of early human development for assisted reproductive technology. Singapore: National University of Singapore; 1993.
22. El Shafie M, Sousa M, Windt ML, Kruger TF. An atlas of the ultrastructure of human oocytes. New York: Parthenon Publishing; 2000.
23. Makabe S, Van Blerkom J, Nottola SA, Naguro T. Atlas of human female reproductive function. ovarian development to early embryogenesis after in vitro fertilization. London: Taylor & Francis; 2006.
24. Ghetler Y, Skutelsky E, Ben Nun I, Ben Dor L, Amihai D, Shalgi R. Human oocyte cryopreservation and the fate of cortical granules. Fertil Steril. 2006;86:210–6.
25. Gualtieri R, Iaccarino M, Mollo V, Prisco M, Iaccarino S, Talevi R. Slow cooling of human oocytes: ultrastructural injuries and apoptotic status. Fertil Steril. 2009;91:1023–34.
26. Sousa M, Cunha M, Silva J, Oliveira E, Pinho MJ, Almeida C, et al. Ultrastructural and cytogenetic analyses of mature human oocyte dysmorphisms with respect to clinical outcomes. J Assist Reprod Genet. 2016;33:1041–57.
27. Fancsovits P, Murber A, Gilán ZT, Rigó Jr J, Urbancsek J. Human oocytes containing large cytoplasmic vacuoles can result in pregnancy and viable offspring. Reprod Biomed Online. 2011;23:513–6.
28. Setti AS, Figueira RC, Braga DP, Colturato SS, Iaconelli Jr A, Borges Jr E. Relationship between oocyte abnormal morphology and intracytoplasmic sperm injection outcomes: a meta-analysis. Eur J Obstet Gynecol Reprod Biol. 2011;159:364–70.
29. Ebner T, Moser M, Sommergruber M, Gaiswinkler U, Shebl O, Jesacher K, et al. Occurrence and developmental consequences of vacuoles throughout preimplantation development. Fertil Steril. 2005;83:1635–40.
30. Wallbutton S, Kasraie J. Vacuolated oocytes: fertilization and embryonic arrest following intra-cytoplasmic sperm injection in a patient exhibiting persistent oocyte macro vacuolization—case report. J Assist Reprod Genet. 2010;27:183–8.
31. Szöllösi D, Mandelbaum J, Plachot M, Salat-Baroux J, Cohen J. Ultrastructure of the human preovulatory oocyte. J In Vitro Fert Embryo Transf. 1986;3:232–42.
32. Familiari G, Heyn R, Relucenti M, Nottola SA, Sathananthan AH. Ultrastructural dynamics of human reproduction, from ovulation to fertilization and early embryo development. Int Rev Cytol. 2006;249:53–141.
33. Motta PM, Nottola SA, Makabe S, Heyn R. Mitochondrial morphology in human fetal and adult female germ cells. Hum Reprod. 2000;15 Suppl 2:129–47.
34. Motta PM, Nottola SA, Familiari G, Makabe S, Stallone T, Macchiarelli G. Morphodynamics of the follicular-luteal complex during early ovarian development and reproductive life. Int Rev Cytol. 2003;223:177–288.
35. Dumollard R, Duchen M, Sardet C. Calcium signals and mitochondria at fertilisation. Semin Cell Dev Biol. 2006;17:314–23.
36. Van Blerkom J. Mitochondrial function in the human oocyte and embryo and their role in developmental competence. Mitochondrion. 2011;11:797–813.
37. Nader N, Kulkarni RP, Dib M, Machaca K. How to make a good egg!: the need for remodeling of oocyte Ca(2+) signaling to mediate the egg-to-embryo transition. Cell Calcium. 2013;53:41–54.
38. Bianchi S, Macchiarelli G, Micara G, Linari A, Boninsegna C, Aragona C, et al. Ultrastructural markers of quality are impaired in human metaphase II aged oocytes: a comparison between reproductive and in vitro aging. J Assist Reprod Genet. 2015;32:1343–58.
39. Otsuki J, Okada A, Morimoto K, Nagai Y, Kubo H. The relationship between pregnancy outcome and smooth endoplasmic reticulum clusters in MII human oocytes. Hum Reprod. 2004;19:1591–7.
40. Sá R, Cunha M, Silva J, Luís A, Oliveira C, Teixeira Da Silva J, et al. Ultrastructure of tubular smooth endoplasmic reticulum aggregates in human metaphase II oocytes and clinical implications. Fertil Steril. 2011;96:143–149.e7.
41. Mateizel I, Van Landuyt L, Tournaye H, Verheyen G. Deliveries of normal healthy babies from embryos originating from oocytes showing the presence of smooth endoplasmic reticulum aggregates. Hum Reprod. 2013;28:2111–7.
42. Van Beirs N, Shaw-Jackson C, Rozenberg S, Autin C. Policy of ivf centres towards oocytes affected by smooth endoplasmic reticulum aggregates: a multicentre survey study. J Assist Reprod Genet. 2015;32:945–50.
43. Shaw-Jackson C, Thomas AL, Van Beirs N, Ameye L, Colin J, Bertrand E, et al. Oocytes affected by smooth endoplasmic reticulum aggregates: to discard or not to discard? Arch Gynecol Obstet. 2016;294:175–84.
44. Vincent C, Pickering SJ, Johnson MH. The hardening effect of dimethylsulphoxide on the mouse zona pellucida requires the presence of an oocyte and is associated with a reduction in the number of cortical granules present. J Reprod Fertil. 1990;89:253–9.
45. Al Hasani S, Diedrich K. Oocyte storage. In: Grudzinskas JG, Yovich JL, editors. Gametes—the oocyte. Cambridge: Cambridge University Press; 1995. p. 376–94.
46. Fuku E, Xia L, Downey BR. Ultrastructural changes in bovine oocytes cryopreserved by vitrification. Cryobiology. 1995;32:139–56.
47. Fuku EJ, Liu J, Downey BR. In vitro viability and ultrastructural changes in bovine oocytes treated with a vitrification solution. Mol Reprod Dev. 1995;40:177–85.
48. Hyttel P, Vajta G, Callesen H. Vitrification of bovine oocytes with the open pulled straw method: ultrastructural consequences. Mol Reprod Dev. 2000;56:80–8.
49. Valojerdi MR, Salehnia M. Developmental potential and ultrastructural injuries of metaphase II (MII) mouse oocytes after slow freezing or vitrification. J Assist Reprod Genet. 2005;22:119–27.
50. Schalkoff ME, Oskowitz SP, Powers RD. Ultrastructural observations of human and mouse oocytes treated with cryopreservatives. Biol Reprod. 1989;40:379–93.

51. Jones A, Van Blerkom J, Davis P, Toledo AA. Cryopreservation of metaphase II human oocytes effects mitochondrial membrane potential: implications for developmental competence. Hum Reprod. 2004;19:1861–6.
52. Borini A, Levi Setti PE, Anserini P, De Luca R, De Santis L, Porcu E, et al. Multicenter observational study on slow-cooling oocyte cryopreservation: clinical outcome. Fertil Steril. 2010;94:1662–8.
53. Ebner T, Moser M, Sommergruber M, Tews G. Selection based on morphological assessment of oocytes and embryos at different stages of preimplantation development: a review. Hum Reprod Update. 2003;9:251–62.
54. Nottola SA, Heyn R, Camboni A, Correr S, Macchiarelli G. Ultrastructural characteristics of human granulosa cells in a coculture system for in vitro fertilization. Microsc Res Tech. 2006;69:508–16.
55. Khalili MA, Maione M, Palmerini MG, Bianchi S, Macchiarelli G, Nottola SA. Ultrastructure of human mature oocytes after vitrification. Eur J Histochem. 2012;56:e38. doi:10.4081/ejh.2012.e38.
56. Practice Committees of American Society for Reproductive Medicine; Society for Assisted Reproductive Technology. Mature oocyte cryopreservation: a guideline. Fertil Steril. 2013;99:37–43.
57. Glujovsky D, Riestra B, Sueldo C, Fiszbajn G, Repping S, Nodar F, et al. Vitrification versus slow freezing for women undergoing oocyte cryopreservation. Cochrane Database Syst Rev. 2014;9:CD010047.
58. Levi-Setti PE, Borini A, Patrizio P, Bolli S, Vigiliano V, De Luca R, et al. ART results with frozen oocytes: data from the Italian ART registry (2005–2013). J Assist Reprod Genet. 2016;33:123–8.
59. Levi Setti PE, Porcu E, Patrizio P, Vigiliano V, de Luca R, d'Aloja P, et al. Human oocyte cryopreservation with slow freezing versus vitrification. Results from the national Italian registry data, 2007–2011. Fertil Steril. 2014;102:90–95.e2.
60. Edgar DH, Gook DA. A critical appraisal of cryopreservation (slow cooling versus vitrification) of human oocytes and embryos. Hum Reprod Update. 2012;18:536–54.
61. Bianchi V, Lappi M, Bonu MA, Borini A. Oocyte slow freezing using a 0.2-0.3 M sucrose concentration protocol: is it really the time to trash the cryopreservation machine? Fertil Steril. 2012;97:1101–7.
62. Parmegiani L, Tatone C, Cognigni GE, Bernardi S, Troilo E, Arnone A, et al. Rapid warming increases survival of slow-frozen sibling oocytes: a step towards a single warming procedure irrespective of the freezing protocol? Reprod Biomed Online. 2014;28:614–23.
63. Stachecki JJ, Willadsen SM. Cryopreservation of mouse oocytes using a medium with low sodium content: effect of plunge temperature. Cryobiology. 2000;40:4–12.
64. Tao T, Del Valle A. Human oocyte and ovarian tissue cryopreservation and its application. J Assist Reprod Genet. 2008;25:287–96.
65. Shanshan G, Mei L, Keliang W, Yan S, Rong T, Zi-Jiang C. Effect of different rehydration temperatures on the survival of human vitrified-warmed oocytes. J Assist Reprod Genet. 2015;32:1197–203.
66. Palmerini MG, Antinori M, Maione M, Cerusico F, Versaci C, Nottola SA, et al. Ultrastructure of immature and mature human oocytes after cryotop vitrification. J Reprod Dev. 2014;60:411–20.
67. Gualtieri R, Mollo V, Barbato V, Fiorentino I, Iaccarino M, Talevi R. Ultrastructure and intracellular calcium response during activation in vitrified and slow-frozen human oocytes. Hum Reprod. 2011;26:2452–60.
68. Bonetti A, Cervi M, Tomei F, Marchini M, Ortolani F, Manno M. Ultrastructural evaluation of human metaphase II oocytes after vitrification: closed versus open devices. Fertil Steril. 2011;95:928–35.
69. Sathananthan AH, Trounson A, Freeman L. Morphology and fertilizability of frozen human oocytes. Gamete Res. 1987;16:343–54.
70. Kornmann B. The molecular hug between the ER and the mitochondria. Curr Opin Cell Biol. 2013;25:443–8.
71. Kroemer G, Galluzzi L, Vandenabeele P, Abrams J, Alnemri ES, Baehrecke EH, et al. Classification of cell death: recommendations of the Nomenclature Committee on Cell Death 2009. Cell Death Differ. 2009;16:3–11.
72. Bang S, Shin H, Song H, Suh CS, Lim HJ. Autophagic activation in vitrified-warmed mouse oocytes. Reproduction. 2014;148:11–9.
73. Bang S, Lee GK, Shin H, Suh CS, Lim HJ. Vitrification, in vitro fertilization, and development of Atg7 deficient mouse oocytes. Clin Exp Reprod Med. 2016;43:9–14.
74. Cheng JP, Lane JD. Organelle dynamics and membrane trafficking in apoptosis and autophagy. Histol Histopathol. 2010;25:1457–72.
75. Shahedi A, Hosseini A, Khalili MA, Norouzian M, Salehi M, Piriaei A, et al. The effect of vitrification on ultrastructure of human in vitro matured germinal vesicle oocytes. Eur J Obstet Gynecol Reprod Biol. 2013;167:69–75.
76. Coticchio G, Dal Canto M, Fadini R, Mignini Renzini M, Guglielmo MC, Miglietta S, et al. Ultrastructure of human oocytes after in vitro maturation. Mol Hum Reprod. 2016;22:110–8.
77. Nikiforaki D, Vanden Meerschaut F, Qian C, De Croo I, Lu Y, Deroo T, et al. Oocyte cryopreservation and in vitro culture affect calcium signalling during human fertilization. Hum Reprod. 2014;29:29–40.
78. Larman MG, Katz-Jaffe MG, Sheehan CB, Gardner DK. 1,2-propanediol and the type of cryopreservation procedure adversely affect mouse oocyte physiology. Hum Reprod. 2007;22:250–9.
79. Ragoonanan V, Less R, Aksan A. Response of the cell membrane-cytoskeleton complex to osmotic and freeze/thaw stresses. Part 2: The link between the state of the membrane-cytoskeleton complex and the cellular damage. Cryobiology. 2013;66:96–104.
80. Vincent C, Garnier V, Heyman Y, Renard JP. Solvent effects on cytoskeletal organization and in-vivo survival after freezing of rabbit oocytes. J Reprod Fertil. 1989;87:809–20.
81. Joly C, Bchini O, Boulekbache H, Testart J, Maro B. Effects of 1,2-propanediol on the cytoskeletal organization of the mouse oocyte. Hum Reprod. 1992;7:374–8.
82. Steinman RM, Mellman IS, Muller WA, Cohn ZA. Endocytosis and the recycling of plasma membrane. J Cell Biol. 1983;96:1–27.
83. Choi JK, Huang H, He X. Improved low-CPA vitrification of mouse oocytes using quartz microcapillary. Cryobiology. 2015;70:269–72.